Journal of Engineering Science and Technology Review 17 (1) (2024) 187 - 198

Research Article

JOURNAL OF
Engineering Science and Technology Review

www.jestr.org

Optimization Analysis of Temperature Control of Massive Concrete Caps Based on Water Cooling of Cooling Pipes

Guanghui Wang[1], Zhonglin Tang[1,*], Yuhao Wang[1], Zhuqiang Tang[2] and Zhenhao Zhang[3, 4]

[1]The College of Civil Engineering and Architecture, Hunan Institute of Science and Technology, Yueyang, 414000, China
[2]Yueyang Tongxiang Transportation Infrastructure Engineering Testing Co., LTD, Yueyang, 414000, China
[3]School of Civil Engineering, Changsha University of Science and Technology, Changsha, 410076, China
[4]Civil engineering department, College of engineering, University of Alaska Anchorage, Anchorage AK, 99508, USA

Received 22 October 2023; Accepted 27 February 2024

Abstract

Massive concrete caps usually adopt cooling pipe water cooling to reduce the negative impact of the hydration heat of cement in construction. However, unreasonable cooling pipe layout, water temperature, and water speed often lead to low cooling efficiency of caps and concrete cracks caused by the excessive temperature difference between the surface and the inside, which can affect the safety and durability of structures. An improved calculation model for massive concrete caps was proposed to reveal the relationship between the transient temperature field of massive concrete caps and the cooling pipe layout and the value of relevant parameters. The proposed model considered the heat of cement hydration, solar radiation, air convection, and the heat exchange of cooling pipes through water. The boundary value conditions were identified through the least-squares method and physical test data, and a prediction model for the transient temperature field of massive concrete based on water cooling through cooling pipes was established. On this basis, the cooling pipe layout and cooling pipe parameters such as spacing, water temperature, and water flow rate were analyzed in accordance with the basic principles of heat conduction. Results demonstrate that, the influence of solar radiation cannot be ignored in the prediction of the transient temperature field of massive concrete caps. The single-circulation side-by-side arrangement of cooling pipes is better than other layout methods. The internal temperature of caps is negatively correlated with the spacing of cooling pipes, but a considerably small spacing of cooling pipes can increase the amount of cooling pipes and the cost of temperature control. Lowering the water temperature can effectively control the temperature difference between the inside and the outside and reduce the risk of concrete cracking. Changing the water flow rate of the cooling pipes can reduce the maximum temperature inside the caps. However, when the water flow rate of the cooling pipes exceeds 2.4 cubic meters per hour, continuing to increase the cooling pipe water flow rate is not effective in reducing the maximum value of the transient temperature field of the caps. This study provides a good reference for temperature control in the construction of massive concrete caps for bridges.

Keywords: Bridge engineering, Massive concrete cap, Hydration heat, Transient temperature field, Parameter analysis

1. Introduction

Long-span bridges are being built in large numbers because of their beautiful shapes, large span capacity, and driving comfort [1]. In such bridges, massive concrete caps are often required to connect large piers and pile group foundations. However, during the construction of massive concrete caps, owing to the heat generated by cement hydration and the influence of external environmental factors, caps crack because of the excessive temperature difference between the inside and the outside, seriously affecting the safety and durability of structures [2-4]. Therefore, numerous engineering and technical personnel have conducted studies on the hydration heat problem of massive concrete structures. Most of the studies on the hydration heat of massive concrete structures started with dams. The U.S. Bureau of Reclamation began to study the temperature control of concrete dams in 1934 [5].

Massive concrete caps are often cooled by cooling pipe water during construction to avoid cracking due to excessive temperature difference between the inside and the outside. The temperature field is determined by factors such as cement hydration heat, cooling pipe water cooling, solar radiation, and heat exchange between the cap and the external environment. However, for massive concrete caps constructed with cofferdams, the temperature field calculation parameters are difficult to determine owing to the impact of the cofferdams blocking wind and sunlight. Accurate analysis of the temperature field of the caps is a great challenge.

Accordingly, scholars have conducted a large number of studies on the hydration thermal effect of massive concrete caps [6-8], but problems remain in the modeling of transient temperature fields that deviate from the actual situation. As the on-site operating environment becomes complex and changeable, how to clarify the processing of boundary value conditions in complex environments and optimize the values of parameters related to water cooling in cooling pipes has become a hot issue that needs to be solved urgently. Therefore, determining how to accurately predict the transient temperature field of massive concrete caps and clarify the reasonable values of boundary conditions has important engineering significance.

To this end, this study uses physical experiments and finite element methods to establish a finite element calculation model for massive concrete caps that can

*E-mail address: zhonglintang1204@163.com
ISSN: 1791-2377
doi:10.25103/jestr.171.22

consider factors such as cement hydration heat, solar radiation, air convection, and water heat exchange in cooling pipes. The form, cooling pipe spacing, water flow temperature, and water flow rate are analyzed parametrically, aiming to predict the transient temperature field of massive concrete caps accurately, thereby providing a reference for the temperature control of such caps.

2. State of the art

Temperature control of massive concrete considers the influence of multiple factors, which can make the temperature field model consistent with reality. However, the accuracy of the values of related parameters of influencing factors affects the calculation accuracy of the temperature field. In recent years, scholars have conducted numerous studies on the transient temperature field during the hydration process of massive concrete.

Studies on the temperature field of massive concrete caps include the following: Haobo Jiang et al. [9] took a suspension bridge cap under construction as the research object and established a calculation model for the hydration heat of the cap. They proposed temperature control measures for air injection cooling of massive concrete internal cooling pipes. However, this temperature control study did not consider solar radiation. Wei Hou et al. [10] took the main pier cap of the Tianninggou Bridge, the second tallest pier in Asia in a loess area, as the research object, established its finite element model, and verified the accuracy of the model through the measured values of the temperature sensors in the cap. However, the measured peak temperature lags behind the calculated value by 60 h. This temperature control study did not mention the influence of solar radiation. Mingshan Geng et al. [11] considered a massive concrete cap as the research object to study the influence of pipe cooling on the temperature control of the cap. They found that water cooling through cooling pipes can significantly reduce the temperature difference between the inside and the outside of the cap and the tensile stress on the concrete surface of the cap, but this study also did not explore the influence of solar radiation. Haidong Huang et al. [12] used the APDL language in Ansys software to establish a refined model for calculating the transient temperature field of concrete caps. However, the results lacked experimental data verification and did not include the influence of solar radiation. Kexin Chen et al. [13] studied the temperature control of the main tower cap of a cross-sea cable-stayed bridge and optimized the pipe diameter, pipe spacing, cooling pipe water temperature, and cooling water flow rate. However, the analysis of cooling pipe parameters in this study was not comprehensive enough; for instance, the cooling pipe layout was not optimized and analyzed.

Results on the temperature field of massive concrete dams are as follows: I. Siva Parvathi et al. [14] conducted a study on the transient temperature field and temperature stress of a roller-compacted concrete gravity dam and discussed the impact of increasing the layered construction thickness of the dam on the temperature thermal stress of the dam body. However, for analyzing the temperature field of dams and considering the influences of solar radiation and stress field, this study was not comprehensive. Zheng Si et al. [15] took a concrete gravity dam as the study object by adopting the thermal-fluid coupling method to conduct parametric analysis on the arrangement of cooling pipes and related parameters, but the solar radiation was not considered in the analysis of the temperature field of the dam body. Eloisa Castilho et al. [16] introduced a calculation model for cement hydration heat and solar radiant heat and applied the results to the Alqueva Dam project. A certain number of temperature sensors were buried to monitor the real-time temperature of the dam body, but the measured values at some measuring points were not consistent with the calculated values of the finite element. Cristian Ponce-Farfan et al. [17] proposed a hydration heat calculation model to simulate and analyze the temperature field during the construction period of a roller-compacted concrete dam under construction. This method considers the influence of climatic conditions and solar radiation on the concrete dam but lacks the verification of test data. Jamil Afzal et al. [18] used a hydration heat model in the form of exponential function to analyze the transient temperature field of a dam. This method can predict the temperature at the middle section of the dam body, but the temperature prediction of the top surface of the dam body is greatly affected by seasonal changes.

The influencing factors of the hydration heat of massive concrete are discussed as follows: Lin Yun et al. [19] studied the adiabatic temperature rise of concrete and the interfacial heat conduction between steel formwork and concrete, but the study did not involve the influence of solar radiant heat on the hydration process of concrete. Tae-Seok Seo et al. [20] proposed a method of setting vertical cooling pipes to control the temperature of slender and massive concrete structures. Although this study demonstrated the importance of pipe cooling, the influence of solar radiation was not considered in component tests. Herbert Abeka et al. [21] studied the temperature rise of 1.1 m^3 concrete blocks by thermocouple resistance. Although the study puts forward the surface area-to-volume ratio as an index to control concrete cracks, it did not consider the actual working environment of massive concrete members, such as their solar radiation. Adek Tasri et al. [22] evaluated the influence of steel, PVC, and PEX materials on the temperature gradient and temperature stress along cooling pipes, but the influence of external factors on temperature stress and transient temperature field should not be ignored. Bruno Ribeiro et al. [23] studied the addition of bagasse fiber, 5% volcanic ash, and other materials to massive concrete. Although this method can effectively decrease the hydration heat, it will also reduce the workability and strength of concrete.

The abovementioned results mainly focus on the prediction of the temperature field of massive concrete caps and concrete dams. Few studies exist on the analysis of factors affecting the hydration heat of massive concrete structures. In particular, research on the accurate prediction of the transient temperature field of massive concrete under the combined effects of water cooling through cooling pipes and the consideration of complex environmental factors, such as solar radiation, is rare. On the basis of the principle of adiabatic temperature rise of concrete and the fundamental principles of heat conduction, this study uses physical experiments and finite element methods to establish a calculation model for massive concrete caps considering cement hydration heat, solar radiation, air convection, and cooling pipe water heat exchange. Through the parameter identification of the boundary value conditions of the experimentally measured values, the changing rules of the transient temperature field of massive concrete caps under different cooling pipe forms, cooling pipe spacing, water temperatures, and water flow rates are discussed, and a cap is formed. The relationship between the transient temperature field of the cap and boundary value conditions, cooling pipe water cooling, and other parameters are established to provide a basis for the temperature control of massive concrete caps.

The remainder of this study is organized as follows. Section 3 describes the adiabatic temperature rise and heat exchange mechanism during the cement hydration process and constructs a calculation method for the transient temperature field of a massive concrete cap that takes into account cement hydration heat, solar radiation, air convection, and cooling pipe water heat exchange. Section 4 analyzes the influence of the relevant parameters of the model's temperature control through the basic principles of heat conduction and the finite element method and obtains the results of the transient temperature of the massive concrete cap in different cooling pipe forms, cooling pipe spacing, water temperatures, and water flows. The last section summarizes this article and gives relevant conclusions.

3. Methodology

The transient temperature field of the bridge's massive concrete cap is determined by factors such as the heat release of cement hydration reaction in the early stage of concrete pouring, water cooling through cooling pipes, solar radiation, and heat exchange with the atmospheric environment, as shown in Figure 1.

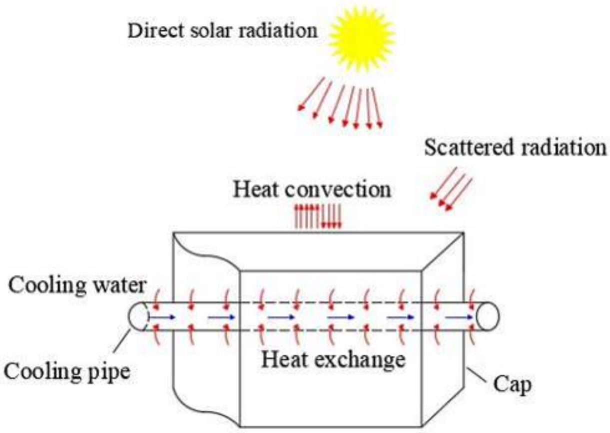

Fig. 1. Heat exchange mechanism of the massive concrete cap

3.1 Assumption

When the transient temperature field of a massive cap is studied, for convenience, the following assumptions are made:

1) During the cement hydration process, concrete changes from a fluid state to a solid state. To facilitate software simulation, this study does not consider the change in the physical state of the massive concrete cap;

2) Concrete is regarded as a homogeneous material, cement is evenly distributed in the concrete, and the hydration degree of the cement in the cap is the same at the same time;

3) When air convection heat exchange is analyzed, the calculation deviation caused by air inhomogeneity is ignored, that is, the temperature field is calculated on the basis of the same convection heat transfer coefficient on the same plane.

3.2 Consideration of the equivalent heat conduction equation of cooling pipes

For calculating the transient temperature field of the cap, the transient heat transfer process in the concrete structure can be expressed by the equivalent partial differential equation of heat conduction (1) [24], which can take into account the factors such as cooling pipe water cooling, air convection, cement hydration heat, and solar radiation in the concrete.

$$\frac{\partial T}{\partial t} = \alpha\left(\frac{\partial^2 T}{\partial x^2} + \frac{\partial^2 T}{\partial y^2} + \frac{\partial^2 T}{\partial z^2}\right) + (T_0 - T_w)\frac{\partial \phi}{\partial t} + \theta_0 \frac{\partial \psi}{\partial t} + \frac{\partial \eta}{\partial t} \tag{1}$$

Where α is the temperature conductivity coefficient, T_0 is the initial temperature of concrete, T_w is the water temperature at the inlet of the cooling pipe, θ_0 is the final adiabatic temperature rise, $\partial\phi / \partial t$ is to consider the influence of the initial temperature difference $T_0 - T_w$, $\partial\psi / \partial t$ is to consider the influence of adiabatic temperature rise, and $\partial\eta / \partial t$ is to consider the influence of external temperature.

3.3 Adiabatic temperature rise

Adiabatic temperature rise can be measured directly by adiabatic temperature rise test, or the hydration heat of cement can be measured first, then the adiabatic temperature rise can be solved. In this study, exponential formula (2) is used to reflect the adiabatic temperature rise of the cap [25].

$$\theta(\tau) = \theta_0(1 - \mathrm{e}^{-m\tau}) \tag{2}$$

where θ_0 is the final adiabatic temperature rise; m is a constant, taking 0.13926.

3.4 Boundary value conditions

The accuracy of boundary value conditions is related to the prediction accuracy of the transient temperature field of massive concrete caps. In the analysis, the underside of the cushion is assumed to have a constant temperature, and its size does not change with time. The boundary value conditions of solar radiation, convection, and cooling pipe heat transfer are determined as follows.

3.4.1 Solar radiation

Cofferdams are usually used in the construction of massive concrete caps in water, and the height of cofferdams is much higher than that of caps. Therefore, the influence of cofferdam shielding on solar radiation duration should be considered when calculating solar radiant heat. As shown in Figure 2, the direct solar angle θ_1 and indirect solar angle θ_2 of the center point of the cap can be solved in accordance with the geometric relationship.

$$\theta_1 = 2\arctan\left(\frac{L}{2} \bullet h_1\right) \tag{3}$$

$$\theta_2 = \frac{\pi}{2} - \arctan\left(\frac{L}{2} \bullet h_1\right) \tag{4}$$

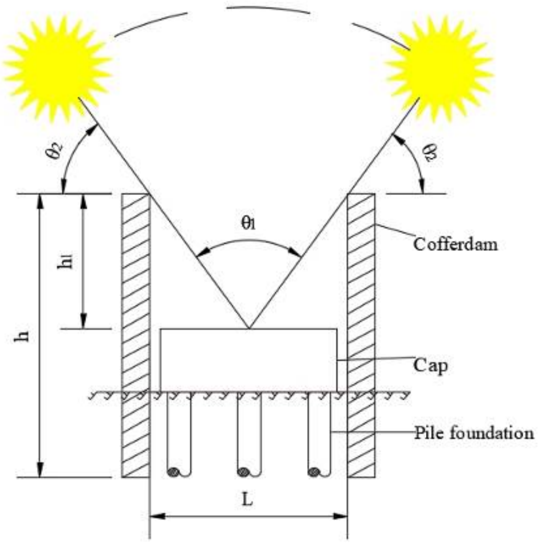

Fig. 2. Calculation diagram for the direct solar angle at the cap center

The solar radiation intensity mainly consists of direct solar radiation and scattered solar radiation, and the absorption of solar radiant heat by the cap surface will be affected by the cloud cover in the atmosphere and the absorption coefficient of the object surface. Therefore, the influence of solar radiant heat on the surface temperature of the cap should be reduced; it can be calculated as follows [26]:

$$I = \alpha\left(I_{DH} + I_{SH}\right)\left(1 - kn\right) \tag{5}$$

where I is the solar radiant heat absorbed by the concrete surface, $\mathrm{kJ/\left(m^2 \cdot h \cdot ^\circ C\right)}$; I_{DH} is the direct solar radiation, $\mathrm{kJ/\left(m^2 \cdot h \cdot ^\circ C\right)}$; I_{SH} is the scattered radiation, $\mathrm{kJ/\left(m^2 \cdot h \cdot ^\circ C\right)}$; α is the solar radiation absorption rate of the concrete surface with a value of 0.5. k is the coefficient of 0.68; n is the cloud cover with a value of 0.2.

Solar radiation intensity can be measured using a photoelectric total solar radiation sensor (Figure 3) [27].

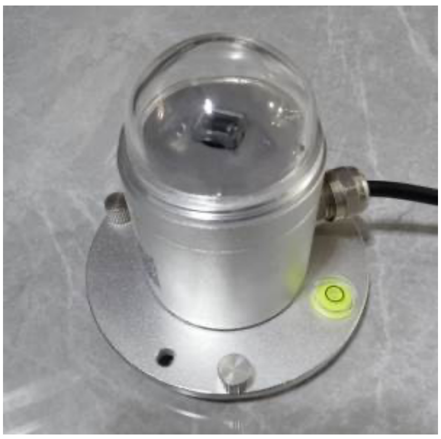

Fig. 3. Photoelectric total solar radiation sensor

3.4.2 Convection

The ambient temperature on the top surface of the cushion and the side of the cap is high because of the influence of the cofferdam, and air convection has a minimal impact on its heat dissipation effect. The influence of air convection can be simplified when calculating the temperature field, while the top surface of the cap mainly contacts with the atmosphere for heat exchange.

The convection coefficient of the top surface of the cap in the atmosphere is related to the wind speed, and it can be calculated in accordance with the heat transfer coefficient expression (6) for rough surfaces [25].

$$\beta = 21.06 + 17.58 v_a^{0.910} \tag{6}$$

In the formula, β is the convection heat transfer coefficient, $\mathrm{kJ/\left(m^2 \cdot h \cdot ^\circ C\right)}$; v_a is the wind speed, $\mathrm{m/s}$.

Wind speed is measured using an anemometer, as shown in Figure 4.

Fig. 4. Anemometer

3.4.3 Heat transfer coefficient of cooling pipes

On the basis of the principle of energy conservation and the theoretical basis of forced convection and in consideration of the influence of factors such as the material and geometric size of the cooling pipe and the water velocity in the cooling pipe, the convection heat transfer coefficient of the cooling pipe can be calculated using Equation (7) [28].

$$h_p = \frac{1}{\dfrac{r_0 \ln \gamma}{a k_p} + \dfrac{\gamma}{1258 r_i^{-0.2} u^{0.8}}} \tag{7}$$

$$\gamma = \frac{r_0}{r_i} \tag{8}$$

In the above formulas, r_0 is the outer diameter of the cooling pipe; r_i is the inner diameter of the cooling pipe, m; k_p is the thermal conductivity of the cooling pipe, taken as 30 $\mathrm{kJ/\left(m \cdot h \cdot ^\circ C\right)}$; u is the water velocity of the cooling pipe, $\mathrm{m/s}$; a is the adjustment coefficient related to the material and geometric size of the cooling pipe.

3.5 Parameter identification

Promptly identifying and correcting m in the adiabatic temperature rise calculation formula in the calculation model, the cooling pipe convection heat transfer coefficient h_p, the adjustment coefficient a, the air convection heat transfer coefficient β, and the solar radiation heat I are necessary to accurately predict the transient temperature field of the massive concrete cap. The least-squares method is used to identify these parameters.

The identification parameter x can be confirmed on the basis of the relationship between the measured value T_i of the key node i (i=1, 2 … n) and the sum of square errors $\bar{e}$ of the calculated value $T_i^{'}$.

$$f(x_i) = \|e\|_2 = \left[\sum_{i=1}^{n} \left| \left(T_i - T_i^{'} \right)^2 \right| \right]^{1/2} \quad (9)$$

The adiabatic temperature rise of concrete can be measured via an adiabatic thermal test. From the test results, the parameter m in Equation (2) is identified, and the identified m value is substituted into Equation (2) to obtain the adiabatic temperature rise curve.

Given a cooling pipe, representative temperature measurement points around the cooling pipe at the platform center are evenly selected. At this time, the influence of air convection heat transfer on its internal temperature measurement points is ignored. Equation (9) is used to identify the values of h_p , and a.

In the same way, the air convection heat transfer coefficient β of the top surface and side of the cap is determined using the identified m , h_p , and a combined with Equation (9). The cofferdam will hinder the air flow rate on the cap side. The influence of the cofferdam needs to be considered in the inverse analysis of the convection heat transfer coefficient on the cap side. The temperature measurement point should be selected as close to the cap bottom as possible. Finally, it is confirmed on the basis of the relationship between the actual measured value T_i of node i and the sum of square errors $\bar{e}$ of the calculated value $T_i^{'}$.

The direct solar radiation node i on the cap surface is selected, and Equation (9) is used to solve for the solar radiation heat I absorbed by the concrete surface. In accordance with Equation (5), the solar radiation absorptivity parameter α on the concrete surface can be identified.

4. Result Analysis and Discussion

4.1 Model verification

4.1.1 Project profile
The main pier cap of a double-layer steel truss continuous beam bridge with a span layout of (60 + 100 + 60) m is used as the research object to verify the correctness of the transient temperature field prediction model proposed in this article. The dimensions of the cap are 11 m in the cross-bridge direction, 9 m in the bridge direction, and 3.5 m in height, as shown in Figure 5. The cap adopts C35 concrete, which is poured and formed at one time. The content of ordinary Portland cement in the concrete is 290 $\mathrm{kg/m^3}$, and the content of mixed materials is 105 $\mathrm{kg/m^3}$. Cooling pipes are arranged at 0.5, 1.5, and 2.5 m along the height direction of the cap to circulate water for cooling. The spacing between cooling pipes is 1.0 m × 1.0 m. The cooling pipes in the middle layer are vertically distributed in the direction of the upper and lower cooling pipes in a "#" shape.

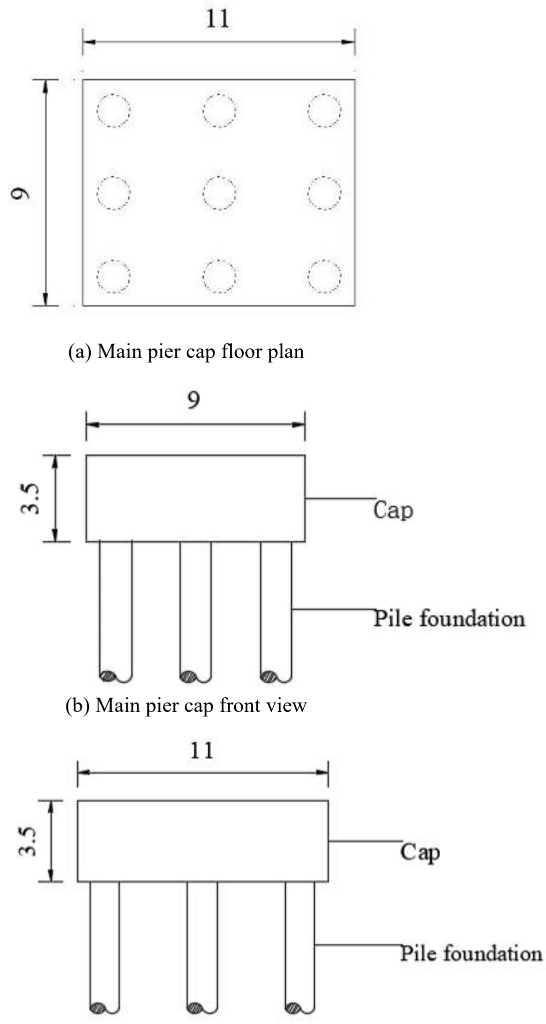

(a) Main pier cap floor plan

(b) Main pier cap front view

(c) Main pier cap side view

Fig. 5. Dimensional drawing of the cap (unit: m)

4.1.2 Concrete material parameters
The material parameters of the cap and cushion concrete are shown in Table 1.

4.1.3 Finite element model
A solid model that can consider the effects of air convection, cooling pipe heat exchange, solar radiation, and other factors, as shown in Figure 6, is established to accurately predict the changes in the temperature field inside the concrete cap. The calculation time is 0-250 h after concrete pouring. The model uses 1D units to simulate cooling pipes and volume units to simulate the cap and cushion concrete. The on-site cap measuring point layout (Figure 7, Figure 8) and temperature acquisition module (Figure 9) are shown below.

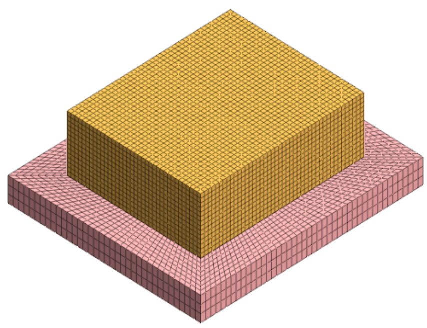

Fig. 6. Finite element model of the massive concrete cap

Table 1. Concrete material parameters

Characteristic	Elastic modulus (Mpa)	Poisson ratio	Density (kg/m^3)	Mass heat capacity ($kJ/(kg\cdot ℃)$)	Thermal conductivity ($kJ/(m\cdot h\cdot ℃)$)	Linear expansion coefficient($1/℃$)
Cap	3.15×10^4	0.2	2500	0.93	9.720	7.7×10^{-6}
Cushion	2.8×10^4	0.2	2500	0.93	9.720	7.7×10^{-6}

Table 2. Cooling pipe material parameters

Outer diameter (m)	Inside diameter (m)	Inlet temperature (℃)	Mass heat capacity ($kJ/(kg\cdot ℃)$)	Flow (m^3/h)	Convection coefficient ($kJ/(m^2\cdot h\cdot ℃)$)
0.048	0.043	15	4.2	1.2	168.27

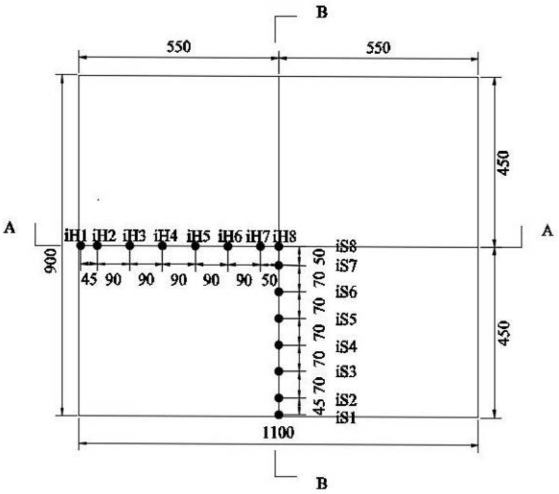

(a) Temperature measuring point layout plan

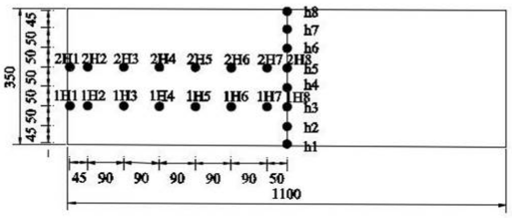

(b) Temperature measuring point layout A-A section diagram

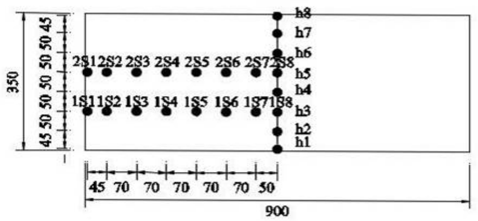

(c) Temperature measuring point layout B-B section diagram

Fig. 7. Temperature measuring point layout diagram (unit: cm)


Fig. 8. On-site cap measuring point layout

4.1.4 Parameter identification

From Equations (7) and (9), the cooling pipe heat transfer coefficient is 168.27 $kJ/(m^2\cdot h\cdot ℃)$.

The cooling pipe material parameters are shown in Table 2. The solar radiation intensity during the cap construction can be obtained using the tested solar radiation heat data and by combining Equations (5) and (9), as shown in Figure 10.

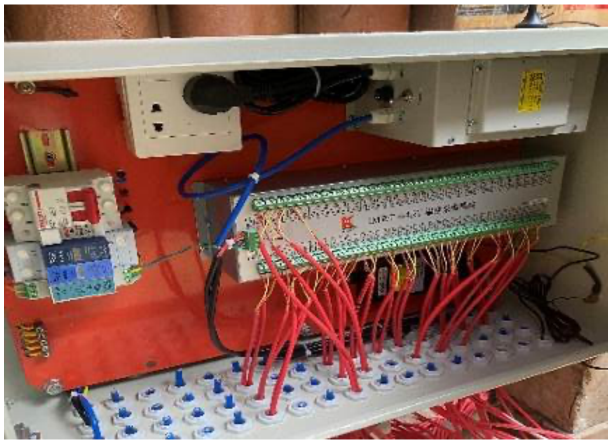
Fig. 9. Temperature acquisition module

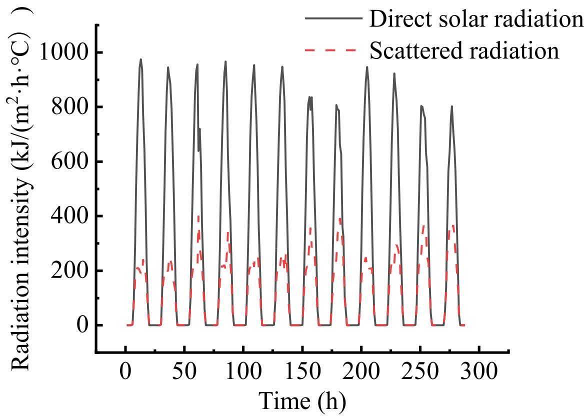

Fig. 10. Solar radiation intensity during cap construction

With the measured wind speed and atmospheric temperature during concrete pouring on the cap, the convection heat transfer coefficient between the top surface of the cap and the atmospheric environment can be obtained in accordance with Equations (6) and (9).

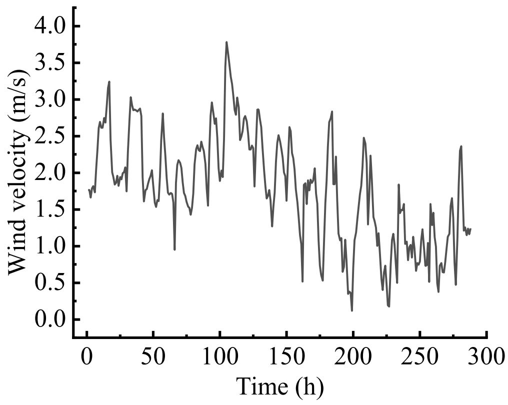

Fig. 11. Wind speed during cap construction

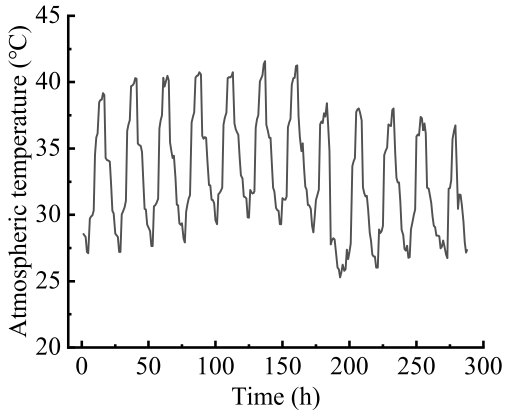

Fig. 12. Atmospheric temperature during cap construction

4.1.5 Comparative analysis of results
To save space, this article selects only the temperature values measured at five points along the height direction of the cap center, namely, h1, h3, h5, h7, and h8, to compare with the calculated values to verify the correctness of the hydration heat analysis model. The comparison between the actual measured values and the calculated values of the temperatures at the measuring points is shown in Figure 13.

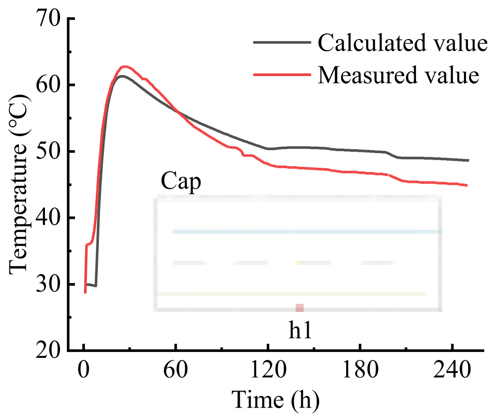

(a) Temperature time history curve of measuring point h1

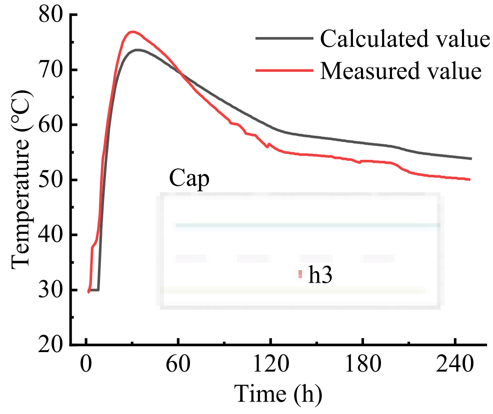

(b) Temperature time history curve of measuring point h3

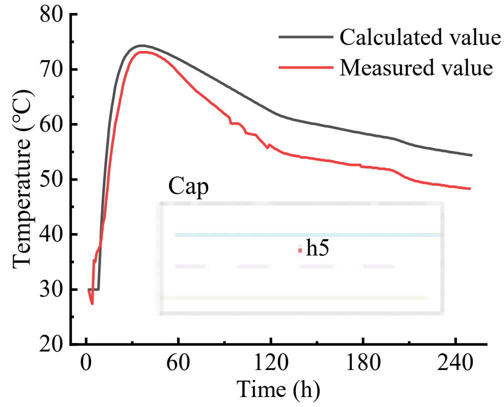

(c) Temperature time history curve of measuring point h5

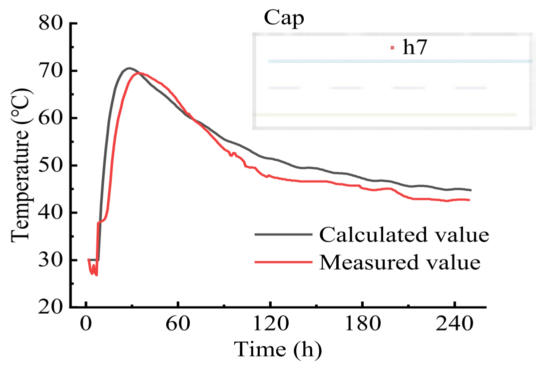

(d) Temperature time history curve of measuring point h7

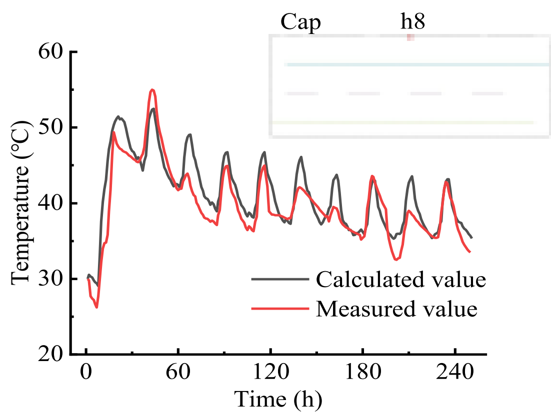

(e) Temperature time history curve of measuring point h8

Fig. 13. Comparison of actual measured values and calculated values of temperatures at measuring points on the massive concrete cap

From Figure 13, the change development trend and peak value of the measured temperature values of the five measuring points along the height direction of the cap center are basically consistent with the calculated values. Therefore, the transient temperature field calculated using this finite element method is scientific and reasonable. The temperature time history curve of measuring point h8 near the cap top is wavy. The main reason is the influence of solar radiation. Appropriate means can be used to control the temperature of h8 point to adjust the temperature difference between the inside and outside and make it within the range indicated by the specification [29].

4.2 Parameter analysis

Factors that affect the transient temperature field of massive concrete caps include cooling pipe layout, cooling pipe spacing, water temperature and flow rate, solar radiation, and external heat exchange. The cooling pipe layout, cooling pipe spacing, water temperature, and water flow rate can be optimized to enhance the cooling effect. This study is based on a transient temperature field calculation model for massive concrete caps and carries out parameter analysis with the above factors.

4.2.1 Parameter analysis

The layout of cooling pipes adopts single- and double-circulation side-by-side and vertical combinations, and the determination of boundary value conditions is the same as that in Section 4.1. The parameter analysis groups are numbered in this section to distinguish the calculation results, as shown in Table 3.

Table. 3. Parameter analysis group numbers for the cooling pipe layout

Case	1	2	3	4	5
Cooling pipe layout	Without cooling pipe	Single-circulation side-by-side	Single-circulation vertical	Double-circulation side-by-side	Double-circulation vertical

The layout of the cooling pipe is shown in Figure 14.

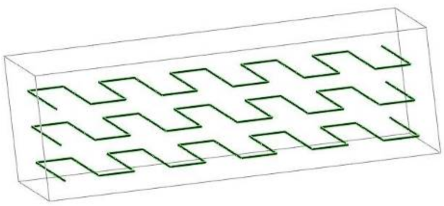

(a) Single-circulation side-by-side arrangement

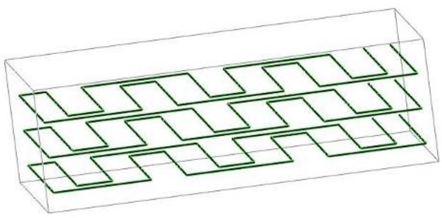

(b) Double-circulation side-by-side arrangement

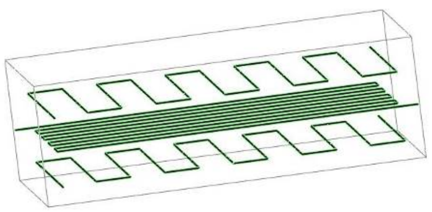

(c) Single-circulation vertical arrangement

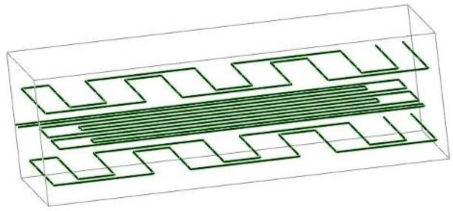

(d) Double-circulation vertical arrangement

Fig. 14. Cooling pipe arrangement

The time history curve of the maximum transient temperature of the cap under the above four cooling pipe arrangements is calculated, as shown in Figure 15. The temperature difference between the maximum transient temperature with and without cooling pipe cooling is shown in Figure 16.

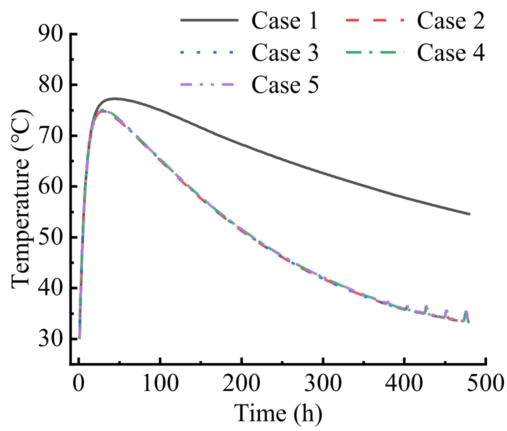

Fig. 15. Maximum transient temperature time history curve of the cap

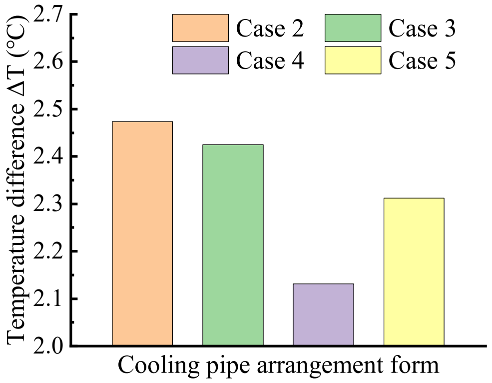

Fig. 16. Comparison diagram for the maximum transient temperature difference between caps with and without a cooling pipe

Under the four combinations of cooling pipe forms, the cooling effect of cooling pipes is in the following order: single-circulation side-by-side ＞single-circulation vertical ＞double-circulation vertical ＞double-circulation side-by-side. Nevertheless, the difference in the maximum transient temperature of concrete among the four ways of installing cooling pipes does not exceed 0.5 ℃. The amount of cooling pipes is shown in Table 4.

Table 4. Amounts of cooling pipes under different cooling pipe layouts

Cooling pipe layout	**Single-circulation side-by-side**	**Single-circulation vertical**	**Double-circulation side-by-side**	**Double-circulation vertical**
Total length of the cooling pipe (m)	297	297	319.5	322.25

Table 4 indicates that the use of cooling pipes and the cost of temperature control of massive concrete caps can be reduced when using single circulation. In consideration of the cooling effect of cooling pipe water cooling and the amount of cooling pipes, the single-circulation side-by-side arrangement of cooling pipe water cooling has a better effect.

4.2.2 Cooling pipe spacing

A comparative analysis is conducted under six working conditions to study the impact of cooling pipe spacing on the effect of cooling pipe water cooling. The conditions include using and not using cooling pipe with cooling pipe spacing of 0.5, 0.75, 1.0, 1.25, and 1.5 m, as shown in Table 5.

Table 5. Cooling pipe spacing

L_D	L_{D-0}	$L_{D-0.5}$	$L_{D-0.75}$	L_{D-1}	$L_{D-1.25}$	$L_{D-1.5}$
Cooling pipe spacing (m)	Without cooling pipe	0.50	0.75	1.00	1.25	1.50

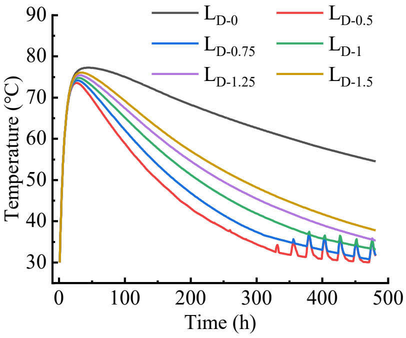

Fig. 17. Maximum temperature time history curve inside the cap

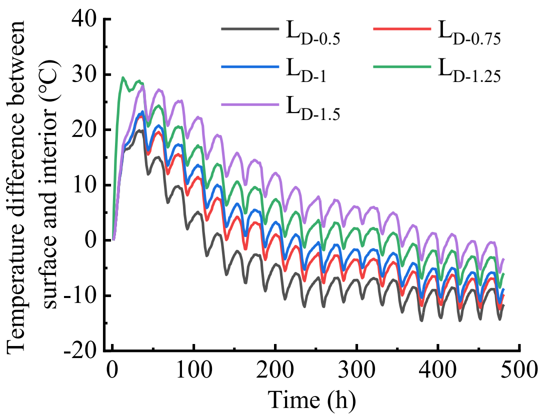

Fig. 18 Temperature difference time history curve between the inside and the outside of the cap

Table 6. Workload of cap temperature control monitoring under various working conditions

Cooling pipe spacing (m)	**0.50**	**0.75**	**1.00**	**1.25**	**1.50**
Temperature monitoring minimum time (h)	220	248	284	319	350
Shortest time for cooling pipe water flow (h)	148	194	230	283	382
Total consumption of cooling pipes (m)	537	394.5	297	249	226.5

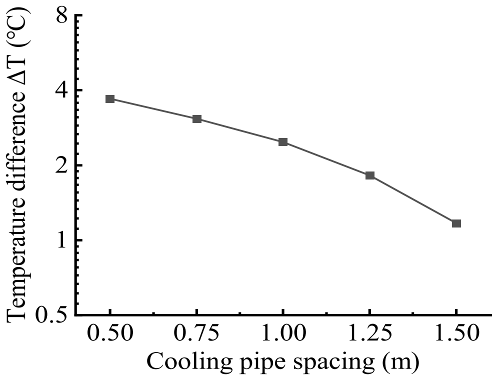

Fig. 19. Maximum temperature difference curve without and with cooling pipe

The time history curve of the maximum transient temperature of the cap under different cooling pipe spacing is presented in Figure 17. The time history curve of the temperature difference between the inside and the outside of the cap under various working conditions is shown in Figure 18.

Figure 17 demonstrates that the smaller the distance between the cooling pipes, the smaller the maximum temperature inside the cap, the lower the temperature difference between the inside and outside, and the shorter the minimum time for water flow through the cooling pipes and the minimum time for temperature control on the cap. In Figure 19, the curve has an inflection point when the cooling pipe spacing is 1 m. Therefore, combined with the water flow efficiency of the cooling pipe, the cooling pipe spacing should be 1.0 m.

4.2.3 Circulating water temperature

To explore the influence of water supply temperature on the cooling effect of cooling pipe water supply, this study analyzes the transient temperature field when cooling water of five temperatures is used to cool the cap. The water temperature is numbered with T_w, as shown in Table 7.

Table 7. Circulating water temperature

T_w	T_{w-0}	T_{w-15}	T_{w-20}	T_{w-25}	T_{w-30}	T_{w-35}
Circulating water temperature (°C)	Without cooling pipe	15	20	25	30	35

Through finite element analysis, the time history curve of the maximum transient temperature of the cap under different water temperatures is obtained, as shown in Figure 20. The time history curve of the temperature difference between the inside and the outside of the cap is depicted in Figure 21.

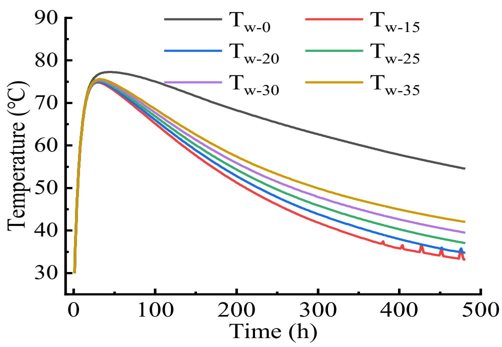

Fig. 20. Time history curve of maximum temperature inside the cap

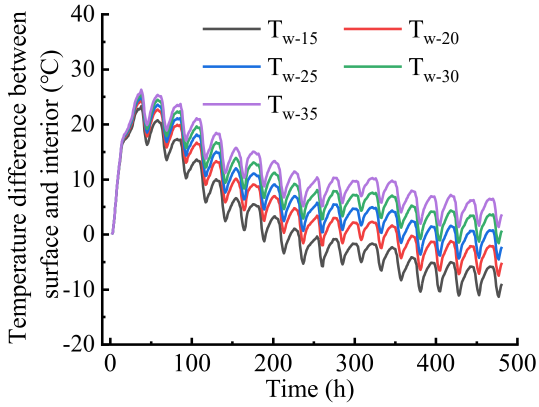

Fig. 21. Temperature difference time history curve between the inside and the outside of the cap

Figures 20 and 21 illustrate that the water supply temperature has a minimal effect on the maximum temperature of the cap but has a greater impact on the cooling stage after the peak temperature of the cap. The lower the water temperature is, the quicker the internal temperature of the cap and the temperature difference between the inside and outside are reduced. Thus, if conditions permit, the temperature of the cooling pipe water can be appropriately lowered.

4.2.4 Circulating water flow analysis

The transient temperature field of the cooling water with five kinds of flow rates on the cap is analyzed to investigate the effect of flow rate on the cooling effect of the cooling pipe. The water flow rate is numbered with L_q, as shown in Table 8.

Table. 8. Circulating water flow

L_q	L_{q-0}	$L_{q-1.2}$	$L_{q-2.4}$	$L_{q-3.6}$	$L_{q-4.8}$	$L_{q-6.0}$
Circulating water flow (m^3/h)	Without cooling pipe	1.2	2.4	3.6	4.8	6.0

The time history curve of the maximum transient temperature of the cap under different flow rates is shown in Figure 22. The maximum temperature difference curve between the conditions without cooling pipe and with different water flows is presented in Figure 23.

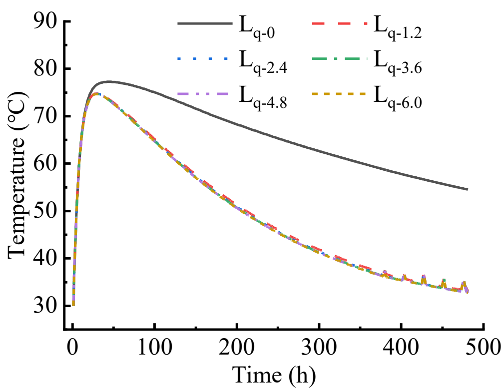

Fig. 22. Time history curve of maximum temperature in the cap

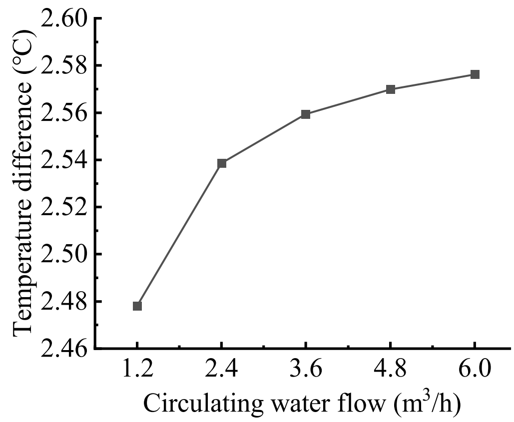

Fig. 23. Maximum temperature difference curve between the conditions without cooling pipe and with different water flows

From Figure 22, the size of the cooling pipe water flow has limited impact on the time history curve of the maximum temperature of the cap. Figure 23 demonstrates that, when the cooling pipe water flow exceeds 2.4 m^3/h, continuing to increase the cooling pipe water flow is not effective in reducing the maximum value of the transient temperature field of the cap.

4.3 Scheme optimization

With regard to cooling pipe spacing, circulating water temperature, and circulating water flow, the following measures can be taken to improve the cooling efficiency of cooling pipe water cooling in massive concrete caps on the basis of the analysis of parameters such as cooling pipe layout: 1) The cooling pipes should be arranged as single-circulation side-by-side. 2) The cooling pipe spacing should be suitable for 1.0 m. 3) The cooling pipe water temperature should be 20℃. 4) The cooling pipe water flow should be fixed at 2.4 m^3/h.

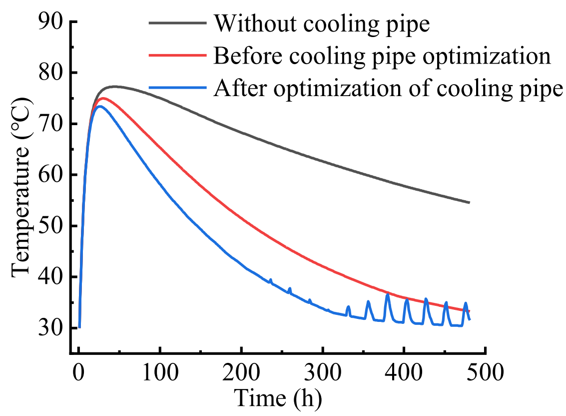

Fig. 24. Maximum transient temperature time history curve of the cap

Table 9. Maximum difference in cap transient temperature, minimum time for temperature monitoring, and shortest time for cooling pipe water flow

	Before cooling pipe optimization	**After cooling pipe optimization**
Maximum transient temperature difference ΔT (°C)	2.43	3.86
Minimum time for temperature monitoring (h)	285	218
Shortest time for cooling pipe water flow (h)	230	144

The above data suggest that the maximum transient temperature of the cap before and after optimization of the cooling pipe are 74.96℃ and 73.40℃, respectively. After the optimization of the cooling pipe, the maximum value of the transient temperature of the cap is 1.56℃ lower than that before the optimization. The temperature monitoring and cooling pipe operation time are also shortened by 67 and 86 h, respectively, compared with those before the cooling pipe optimization. The cooling effect of the transient temperature field of the cap after the cooling pipe optimization is significantly better than that before the cooling pipe optimization.

5. Conclusions

To accurately predict the transient temperature field of a massive concrete cap and reveal the relationship between the transient temperature field of the massive concrete cap, the boundary value conditions, and the parameters related to the water cooling of the cooling pipe, this study established a physical model for the temperature control of massive concrete caps. A combination of numerical simulation technology and experimental research was used to analyze the cooling pipe layout, cooling pipe spacing, and water temperature of the cooling pipes of massive concrete caps, and the water flow was examined. The following conclusions could be drawn:

1) Solar radiation has a significant impact on the temperature difference between the inside and the outside of the cap. Therefore, the influence of solar radiation must be considered when calculating the transient temperature field during the construction period of massive concrete caps.

2) When cooling water through the cooling pipe, the layout of the cooling pipe and the flow rate of the cooling pipe have limited influence on the maximum value of the transient temperature of the cap and the temperature difference between the surface and the inside. Reducing the distance between the cooling pipes and the water temperature can effectively decrease the maximum temperature of the cap and the temperature difference between the surface and the inside of the cap.

3) The optimized cooling scheme of the cooling pipe makes the cooling effect of the cap remarkable and can shorten the temperature monitoring time by 67 h and the cooling pipe working time by 86 h, thus further improving the construction efficiency.

This study combined field test and numerical simulation to propose an optimization method for cooling massive concrete caps with circulating water based on cooling pipes during construction. The transient temperature field calculation model for massive concrete caps, which can consider cement hydration heat, solar radiation, air convection, and heat exchange through cooling pipes, is close to the field practice. It has a certain reference for temperature control in the construction of massive concrete caps. Because the temperature control optimization of massive concrete caps in this study only analyzed the whole process of cooling through the cooling pipe of a massive concrete cap, the transient temperature field of massive concrete caps under nonuniform water velocity and temperature will be actively explored in future work.

References

[1] W. Q. Mao and X. W. Hu, "Latest developments and prospects for Long-Span bridges in China," *Bridg. Constr.*, vol. 50, no. 01, pp. 13-19, Mar. 2020.
[2] H. Chen and F. Y. Han, "Factors and controlling measures caused by the temperature cracking of mass concrete," *Concrete*, vol. 2, pp. 74-75, Feb. 2006.
[3] T. Zhao, Y. T. Jiao, Y. K. Zhang, and L. L. Hou, "Study on cracking mechanism of gravity dam based on Macro-Micro model," *Water Resour. Power*, vol. 41, no. 11, pp. 65-68+9, Nov. 2023.
[4] Y. H. Hu, "Some insights on temperature crack control in reinforced concrete structures," *Build. Struct.*, vol. 53, no. 16, pp. 98-104+97, Aug. 2023.
[5] H. Z. Wang, "Heat dissipation problem and calculation method of concrete," *China Water Resour.*, vol. 11, pp. 3-7, Jun. 1956.
[6] F. C. Song and C. Liu, "Hydration thermal analysis of mass concrete considering pipe cooling," *J. Shenyang Jianzhu Univ. (Nat. Sci.)*, vol. 31, no. 1, pp. 95-101, Jan. 2015.
[7] X. W. Shang, S. M. Xiao, W. Q. Zheng, Y. Yang, and K. Ma, "Hydration kinetics analysis of cementitious paste composites produced by binary and ternary binder materials for potential use in massive concrete structures," *Case Stud. Constr. Mater.*, vol. 18, pp. 1-12, Jun. 2023.
[8] X. M. Wan, H. Li, X. P. Che, P. Z. Xu, C. J. Li, and Q. Yu, "A study on the application of recycled concrete powder in an Alkali-Activated cementitious system," *Processes*, vol. 11, no. 1, pp. 203-203, Jan. 2023.
[9] H. B. Jiang, Z. S. Song, W. H. Zhu, and D. H. Yan, "Research on temperature control of wind cooling for mass concrete of pile cap," *J. China & Foreign Highw.*, vol. 41, no. 5, pp. 161-163, Oct. 2021.
[10] W. Hou, Y. F. Song, and C. Ma, "Time varying temperature effect of hydration heat of mass concrete based on pipe cooling system," *J. Chang'an Univ. (Nat. Sci. Ed.)*, vol. 41, no. 4, pp. 65-77, Jul. 2021.
[11] M. S. Geng, E. J. Lin, J. B. Lu, and B. Fu, "Hydration heat analysis and temperature control of mass concrete pile cap," *Concrete*, vol. 9, pp. 50-55, Sep. 2021.
[12] H. D. Huang, M. Y. Xu, M. Li, and C. Luo, "Transient temperature field and fine analysis model of concrete cap containing cold pipe," *J. Chongqing Jiaotong Univ. (Nat. Sci.)*, vol. 41, no. 8, pp. 102-111, Aug. 2022.
[13] K. X. Chen, M. L. He, L. Jin, and L. Tao, "Pipe cooling optimization of the mass marine concrete temperature fields for the main tower cap of the Zhoudai Sea-crossing Cable-stayed bridge," *Eng. Adv.*, vol. 3, no. 3, pp. 210-215, Jul. 2023.
[14] I. S. Parvathi and S. Shehanaz, "Thermal transient stress analysis in RCC dam construction," *Mater. Today: Proc.*, vol. 02, no. 329, pp. 1-11, Mar. 2023.
[15] Z. Si, S. L. Wang, Z. X. Wang, and L. F. Xin, "Simulation analysis of mass concrete with cooling pipes based on heat-fluid coupling method," *J. Xi'an Univ. Technol.*, vol. 33, no. 3, pp. 270-275, Sep. 2017.
[16] E. Castilho, N. Schclar, C. Tiago, and M. B. Farinha, "FEA model for the simulation of the hydration process and temperature evolution during the concreting of an arch dam," *Eng. Struct.*, vol. 174, pp. 165-177, Jul. 2018.
[17] C. Ponce-Farfán, D. Santillán, and M. A. Toledo, "Thermal simulation of rolled concrete dams: Influence of the hydration model and the environmental actions on the thermal field," *Water*, vol. 12, no. 3, pp. 1-19, Mar. 2020.
[18] J. Afzal, Z. Yihong, M. Aslam, and M. Qayum, "A study on thermal analysis of under-construction concrete dam," *Case Stud. Constr. Mater.*, vol. 17, pp. 1-6, Dec. 2022.
[19] Y. Lin and H. L. Chen, "Thermal analysis and adiabatic calorimetry for early-age concrete members," *J. Therm. Anal. Calorim.*, vol. 122, no. 2, pp. 937-945, Nov. 2015.
[20] T. S. Seo, S. S. Kim, and C. K. Lim, "Experimental study on hydration heat control of mass concrete by vertical pipe cooling method," *J. Asian Archit. Build. Eng.*, vol. 14, no. 3, pp. 657-662, Sep. 2015.
[21] H. Abeka, S. Agyeman, M. Adom-Asamoah, and R. R. Hussain, "Thermal effect of mass concrete structures in the tropics:

Experimental, modelling and parametric studies," *Cogent Eng.*, vol. 4, no. 1, pp. 1-18, Jan. 2017.

[22] A. Tasri and A. Susilawati, "Effect of material of post-cooling pipes on temperature and thermal stress in mass concrete," *Structures*, vol. 20, pp. 204-212, Aug. 2019.

[23] B. Ribeiro, T. Yamamoto, and Y. Yamashiki, "A study on the reduction in hydration heat and thermal strain of concrete with addition of Sugarcane Bagasse Fiber," *Materials*, vol. 13, no. 13, pp. 1-14, Jul. 2020.

[24] B. F. Zhu. The equivalent heat conduction equation of pipe cooling in mass concrete considering influence of external temperature," *J. Hydraul. Eng.*, vol. 3, pp. 49-54, Mar. 2003.

[25] B. F. Zhu, *Thermal Stresses and Temperature control of Mass Concrete*. Beijing, CHN: China Water & Power Press, 2012.

[26] D. W. Hou, J. Zhang, and Y. Gao, "Simulation of temperature field of concrete pavement at early-age," *Eng. Mech.*, vol. 29, no. 6, pp. 151-159, Jun. 2012.

[27] F. Zhang and J. Y. Liu, "Study on temperature distribution of three-cell box girder during the hydration process," *J. Therm. Anal. Calorim.*, vol. 148, pp. 2629-2643, Jan. 2023.

[28] Z. G. Lu and X. X. Wang, "Analysis of temperature control for mass concrete bearing platform with water pipe cooling considered," *J. Railway Sci. Eng.*, vol. 12, no. 5, pp. 1172-1178, Oct. 2015.

[29] *Technical code for temperature measurement and control of mass concrete*, GB/T51028-2015, Ministry of Housing and Urban-Rural Development of the People's Republic of China, Beijing, China, Dec. 2015.